GeoStorage

Vol. 2, No. 2, p. 98-105, 2026

Research article

Experimental Investigation of Caprock Wettability and Helium-water Interfacial Tension: Implications for Structural Gas Geo-storage Capacity Estimation

Yuetong He[1], Shouceng Tian[2], Xianzhi Song[1], Gensheng Li[1], Gang Wang[3], Niklas Heinemann[4,5], Mujahid Ali[6], Faisal Ur Rahman Awan[6], Stefan Iglauer[6], Bin Pan[1]*

[1] *State Key Laboratory of Petroleum Resources and Engineering, China University of Petroleum (Beijing), Beijing 102249, China*
[2] *College of Petroleum, China University of Petroleum (Beijing) at Karamay, Karamay 834000, China*
[3] *Institute of GeoEnergy Engineering, Heriot-Watt University, Edinburgh EH14 4AS, United Kingdom*
[4] *Institut UB-Geomodels, Facultat de Ciències de la Terra, Universitat de Barcelona, c/Martí i Franquès s/n, 08028, Barcelona, Spain*
[5] *Departament de Dinàmica de la Terra i de l'Oceà, Facultat de Ciències de la Terra, Universitat de Barcelona, c/Martí i Franquès s/n, 08028, Barcelona, Spain*
[6] *Centre for Sustainable Energy and Resources, Edith Cowan University, 270 Joondalup Drive, Joondalup, Australia*

Keywords:
Caprock
wettability
gas-water interfacial tension
helium
geostorage capacity

Cited as:
He YT, Tian SC, Song XZ, et al. 2026. Experimental Investigation of Caprock Wettability and Helium-water Interfacial Tension: Implications for Structural Gas Geo-storage Capacity Estimation. *GeoStorage*, 2(2), 98-105.
https://doi.org/10.46690/gs.2026.02.01

Abstract:
Helium is a strategic but non-renewable reserve which has important applications in advanced technology areas. Its supply-demand balance is vulnerable to international geopolitics, thus indispensable to store large amounts of helium and one promising storage option is helium geo-storage in porous reservoirs. In this scenario, caprock wettability (characterized by advancing and receding water contact angles, θ_A and θ_R) and helium-water interfacial tension are two most important parameters determining structural helium geo-storage capacity. However, relevant experimental data are seriously lacking. Therefore herein, we measured these two parameters and estimated the geo-storage capacity at subsurface conditions. We demonstrated that 1) clay-rich, organic-rich and carbonate-rich caprocks ranged from completely to strongly water-wet ($\theta_R \sim 0°-35°$), from strongly water-wet to intermediate-wet ($\theta_A \sim 20°-78°$), and from strongly to weakly water-wet ($\theta_A \sim 17°-53°$) states, respectively; 2) helium-water interfacial tension fluctuated around 68 – 73mN/m, irrelevant of pressure; and 3) structural gas geo-storage capacity varied up to twenty times with caprock wettability. This work provides fundamental data for helium geo-storage, thus enabling long-term helium supply-security worldwide.

1 Introduction

Helium is a strategic reserve and a critical raw material, which is vital to healthcare, electronics, aerospace, military, communications, magnetic resonance imaging, and material science (Anderson, 2018; Hurd et al., 2012; Nuttall et al., 2012; Siddhantakar et al., 2023). Furthermore, helium is a non-renewable resource, primarily formed in the Earth's crust by the decay of radioactive uranium (U^{238}) and thorium (Th^{234}) (Ballentine et al., 2002; Cheng et al., 2023). However, helium is a rare element which is mainly obtained as a by-product of natural gas production in the USA, Qatar, Algeria, Russia, Canada, and Australia (Gluyas, 2023), thus the global helium supply-demand balance is extremely vulnerable to international geopolitics (Siddhantakar et al., 2023). For example, Qatar previously had accounted for up to 32% of the global helium supply; on June 5, 2017, neighbouring countries initiated a trade embargo of Qatar; this raised serious concerns about helium

Yandy Scientific Press

* Corresponding author.
E-mail address: 2024012334@student.cup.edu.cn (He YT); tscsydx@163.com (Tian SC); songxz@cup.edu.cn (Song XZ); ligs@cup.edu.cn (Li GS); G.Wang@hw.ac.uk (Wang G); n.heinemann@ub.edu (Heinemann N); mujahid.ali@ecu.edu.au (Ali M); f.awan@ecu.edu.au (Awan FUR); s.iglauer@ecu.edu.au (Iglauer S); binpan@cup.edu.cn (Pan B)
3080-8812
Received Feb. 10, 2026; revised Feb. 21, 2025; accepted Feb. 26, 2026; available online Mar. 29, 2026.

shortage and price increases in the United States, though the US was the leading supplier of helium in the world (Anderson, 2018).

Therefore, it is necessary to store large amounts of helium, to de-risk helium supply. Analogous to H_2, CH_4, and CO_2 geo-storage (Pan et al., 2017, 2021; Heinemann et al., 2021; Pan et al., 2023, 2024, 2025), an opportunity with great potential for large-scale helium storage is to store helium in subsurface porous reservoirs (Rapatskaya et al., 2020). For example, in the 1960s the US Bureau of Mines launched the first helium storage project in the Cliffside sandstone Reservoir, Texas, and the predicted helium storage capacity was up to 41.5 billion cubic feet (10.7 billion cubic feet was already in storage by 1966) (Tade, 1967). In such a conventional reservoir, an ultra-low permeability caprock (e.g., shales and carbonates) prevents the gas from escaping upwards out of the reservoir (Espinoza et al., 2017; Song, 2023). However, such a caprock is still permeable and thus in principle gas still can migrate through it – only capillary forces hold the gas back (Iglauer et al., 2021). The magnitude of these capillary forces depends on the caprock pore size and wettability, and the helium-water interfacial tension (Pan et al., 2021). However, while the caprock pore size is reasonably well understood (Nelson, 2009), the caprock wettability and the helium-water interfacial tension are currently unknown.

Technically, the most commonly-used method for wettability quantification is the sessile water droplet contact angle [including advancing (θ_A) and receding (θ_R)] measurements (Pan et al., 2021). When θ_A or θ_R is 0°, 0°−50°, and 50°−70°, it corresponds to completely, strongly, and weakly water-wet, respectively; when θ_A or θ_R is 70° − 100°, it is considered as intermediate-wet (Iglauer et al., 2021). Meanwhile, the most routine approach for gas-water interfacial tension characterization is the pendent droplet method measurement(Pan et al., 2020; Berry et al., 2015).

Therefore herein, for the first time, we experimentally investigated the caprock wettability and the helium-water interfacial tension via water contact angle and interfacial tension measurements at subsurface conditions, and theoretically estimated the gas geo-storage capacity accordingly. We demonstrated that clay-rich and carbonate-rich caprocks are water-wet and thus in principle efficient helium seals, while organic-rich caprocks are gas-wet and thus unfavorable for helium geo-storage. This work provides fundamental data for helium geo-storage, aiding in the implementation of long-term helium supply-security globally.

2 Methodology

2.1 Caprock samples

We selected six caprock samples (Table 1) and evaluated their helium wettability. The petrophysical properties [i.e., total organic carbon (TOC) content, mineral composition, surface roughness, and average pore radius] of these samples were thoroughly characterized. Specifically, TOC content was measured by rock eval analysis using a Leco CS-230 instrument, following the Standard GB/T 19145-2022; mineral composition was identified by X-ray diffraction measurement using a Rigaku Ultima IV XRD instrument, following the Standard SY/T 5163-2018; surface roughness was quantified by an AFM DSE 95–200 AFM instrument; average pore radius was determined by low-pressure gas adsorption using a Micrometrics Tristar II 320 instrument.

As shown in Table 1, shale 1 and 2 were clay-rich with the clay content up to 47.2 wt.% and 79 wt.%, respectively, while shale 3 and 4 were organic-rich with the TOC content up to 5.99 wt.% and 10 wt.%, respectively; the dominant mineral in the carbonate-rich limestone sample was dolomite (up to 83.1 wt.%). The Barrett-Joyner-Halenda average pore radius of shale 1, shale 4 and limestone was 5, 20 and 6 nm respectively. We did not have enough samples for direct pore size distribution measurements for shale 2 and shale 3 sample. However, shale 3 was reported to range from 1.5 to 10 nm in diameter (Liang et al., 2021); The root-mean-square surface roughnesses of these caprock substrates were all below 1000 nm, under which conditions surface roughness has a negligible influence on the contact angles measured (Al-Yaseri et al., 2016).

2.2 Contact angle and interfacial tension measurements

The caprock samples were cut into cuboid substrates (with a dimension of 20 mm × 13 mm × 2 mm), rinsed with ethanol and then dried at 80 °C in an oven for 10 mins. To mimic realistic subsurface conditions, and to avoid any artificial surface oxidation, air plasma exposure was not applied to these substrates (Pan et al., 2020). Subsequently, advancing (θ_A) and receding (θ_R) deionized water contact angles in helium atmosphere were measured on these caprocks by the tilting plate method (Lander et al., 1993), at various helium geo-storage conditions (i.e., 2.5, 5, 10, 15 and 20 MPa at 50 °C).In addition, helium-water interfacial tension ($\gamma_{H_e-H_2O}$) was measured at the same geothermal conditions as the contact angle measurements, using the pendant droplet method (Berry et al., 2015).

Based on replicate measurements, the standard deviations of the θ_A and θ_R ranged from ±3° to ±10° depending on various pressure and substrate conditions; while the standard deviations of the $\gamma_{H_e-H_2O}$ was $\pm 1 mN/m$.

2.3 Helium column height estimation

The maximum helium column height (hmax) which can be permanently stored beneath the caprock was estimated with a capillary force - buoyancy force balance,

$$h_{max} = \frac{2\gamma_{H_e-H_2O} cos\theta_r}{(\rho_{H_2O} - \rho_{H_e})gr} \quad (1)$$

where ρ_{H_2O} and ρ_{He} are the water and helium density, respectively, kg/m^3, collected from the National Institute of Standards and Technology Chemistry WebBook (https://webbook.nist.gov/chemistry/fluid/); g is the gravity constant, 9.81 N/kg; r is the average pore radius, nm; θ_r and γ_{He-H_2O} are the receding contact angle and helium-water interfacial tension, respectively, as above-mentioned. Furthermore, a hydrostatic gradient of 1 MPa/100 m was assumed (Nunn, 1996).

3 Results and Discussion

Tab. 1 Petrophysical properties of the six caprock samples used

Sample	TOC [wt.%]	Mineral composition [wt.%]	Surface roughness [nm]	Average pore radius [nm]
Shale 1 (clay-rich)	0.56	Quartz: 38.5 Illite: 27.8 Calcite: 9.2 Chlorite: 9.1 Illite-smectite interlayer: 7.2 Kaolinite: 3.1 Siderite: 2.1 Pyrite: 1.2 Gypsum: 1.1 K-feldspar: 0.7	356	5
Shale 2# (clay-rich)	1.3	Illite: 57 Quartz: 24 Chlorite: 19	220	/
Shale 3 (organic-rich)	5.99	Quartz: 28.6 Anorthose: 11.8 Dolomite: 4.9 Pyrite: 4.4 Illite: 20.7 Kaolinite: 6.4 Chlorite: 7.3 Illite-smectite: 15.8	440	/
Shale 4# (organic-rich)	10	Ankerite: 45.1 Anorthose: 17.3 Calcite: 13.4 Aragonite: 10.7 Quartz: 6.9 Pyrite: 6.6 Clay: <1	129	20
Limestone (dolomite-rich)	1.22	Quartz: 16.4 Dolomite: 83.1 Calcite: 0.3 Illite: 0.2	540	6
Calcite	0.24	Calcite: 99.4 Dolomite: 0.3 Soft marble: 0.2 Quartz: 0.1	2	/

3.1 Helium wettability of caprocks

Helium wettability of caprocks demonstrated complex wetting behaviors, Figure 1 and Table 2.

Figure 1. (a) Advancing and (b) receding water contact angles of the helium-water-caprock systems at various pressures, measured at 50°C . The dots are the experiment data and the lines are used for guiding eyes.

Once a water droplet dispensed onto the shale 1 surface, it would spread into a flat water film immediately (see SI-Video 1), regardless of pressure change, thus θ_A and θ_R always remained 0°, indicating a completely water-wet state of shale 1;

Tab. 2 Advancing and receding water contact angles of helium on caprocks as a function of pressure at 50 ºC.

Caprock	Pressure [MPa]	Advancing [°]	Receding [°]
Shale 1	5	0	0
	10	0	0
	15	0	0
	20	0	0
Shale 2	5	26	20
	10	31	27
	15	30	28
	20	39	35
Shale 3	5	30	20
	10	36	20
	15	37	32
	20	54	43
Shale 4	2.5	68	59
	5	68	63
	10	84	76
	15	85	78
	20	85	77
Limestone	5	29	26
	10	33	26
	15	32	28
	20	55	53
Calcite	5	30	20
	10	31	17
	15	31	18
	20	32	20

Tab. 3 Helium-water interfacial tension as a function of pressure at 50 ºC.

Pressure [MPa]	Interfacial tension [mN/m]
0.1	72
5	68
10	72
15	73
20	70

in contrast, when pressure increased from 5 MPa to 20 MPa, θ_A and θ_R on shale 2 increased from 26° to 39° and from 20° to 35°, respectively, indicating a strongly water-wet state. Clay mineral contents (i.e., 47.2 wt.% and 76 wt.%, respectively) were very high in shale 1 and 2 (compare Table 1); we therefore conclude that clay-rich caprocks are strongly hydrophilic at helium geo-storage conditions, qualitatively consistent with the H_2, CH_4 and CO_2 wettability of clays and clay-rich caprocks at gas geo-storage conditions (Hosseini et al., 2022; Pan et al., 2019). The specific wettability differences between shale 1 and 2 are attributed to the different TOC content (0.56 wt.% versus 1.3 wt.%), clay content/type (27.8 wt.% illite + 9.1 wt.% chlorite + 7.2 wt.% illite-smectite interlayer + 3.1 wt.% kaolinite versus 57 wt.% illite + 19 wt.% chlorite) and quartz content (38.5 wt.% versus 24 wt.%), again see Table 1 and also compare (Pan et al., 2020; Arif et al., 2017). As is known, a higher TOC leads to a larger contact angle (thus a weaker hydrophilicity) and a TOC content threshold exists between 1.2 wt.% and 1.3 wt.%,

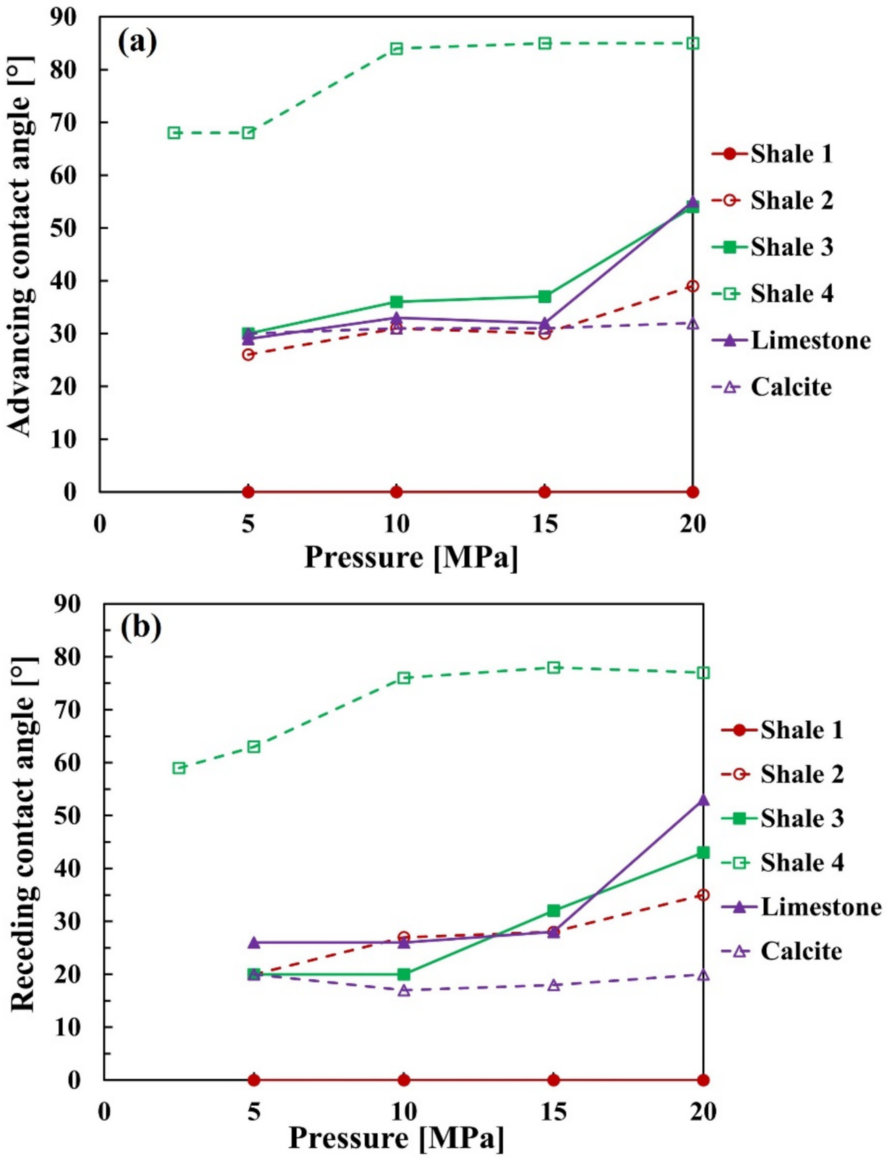

Fig. 1 Advancing (a) and receding (b) water contact angles of the helium-water-caprock systems at various pressures, measured at 50 °C. The dots are the experimental data and the lines are used for guiding the eye

leading to a drastic contact angle shift from 0° to 50° (Pan et al., 2020); clay and clean quartz are usually completely or strongly water-wet (Pan et al., 2019; Iglauer et al., 2021). Thus, it is reasonable that shale 1 is completely water-wet and shale 2 is strongly water-wet in this work.

In comparison, θ_A and θ_R on shale 3 increased from 30° to 54° and from 20° to 43°, respectively, when pressure increased from 5 *MPa* to 20 *MPa*, indicating a transition from strongly to weakly water-wet states with increasing pressure (and thus increasing storage depth) (Iglauer et al., 2021); furthermore, θA and θR on shale 4 increased from 68° to 85° and from 59° to 85°, respectively, when pressure increased from 2.5 MPa to 20 MPa, indicating a transition from weakly water-wet to intermediate-wet states. In shale 3 and 4 samples, TOC contents are relatively high (5.99 wt.% and 10 wt.%) and water-wet minerals [e.g., quartz and clay (Iglauer , 2017; Pan et al., 2020, 2019) are relatively lean, therefore, weakly water-wet to intermediate-wet behaviors were observed in these organic-rich caprocks at helium geo-storage conditions.

Further, limestone and calcite caprocks were strongly to weakly water-wet at helium geo-storage conditions. Specifically, when pressure increased from 5 *MPa* to 20 *MPa*, $\theta_A$and θ_R on limestone (which is dolomite-rich with content up to 83.1 wt.%) increased from 29° to 55° and from 26° to 53°, respectively; while θ_A and θ_R on calcite remained 31° ± 1° and 19° ± 2°, respectively. In contrast, θ_A and θ_R for brine (2 wt.% NaCl + 1 wt.% KCl) contact angle in the hydrogen environment at the surface of Indiana limestone (with calcite content up to 97 wt.%) were measured as 70° and 67°, respectively at 8.27 *MPa*, indicating weakly water-wet state (Hosseini et al., 2023); θ_A and θ_R for deionized water droplet at the surface of kerogen was 30° larger for hydrogen than for helium (Pan et al., 2024).

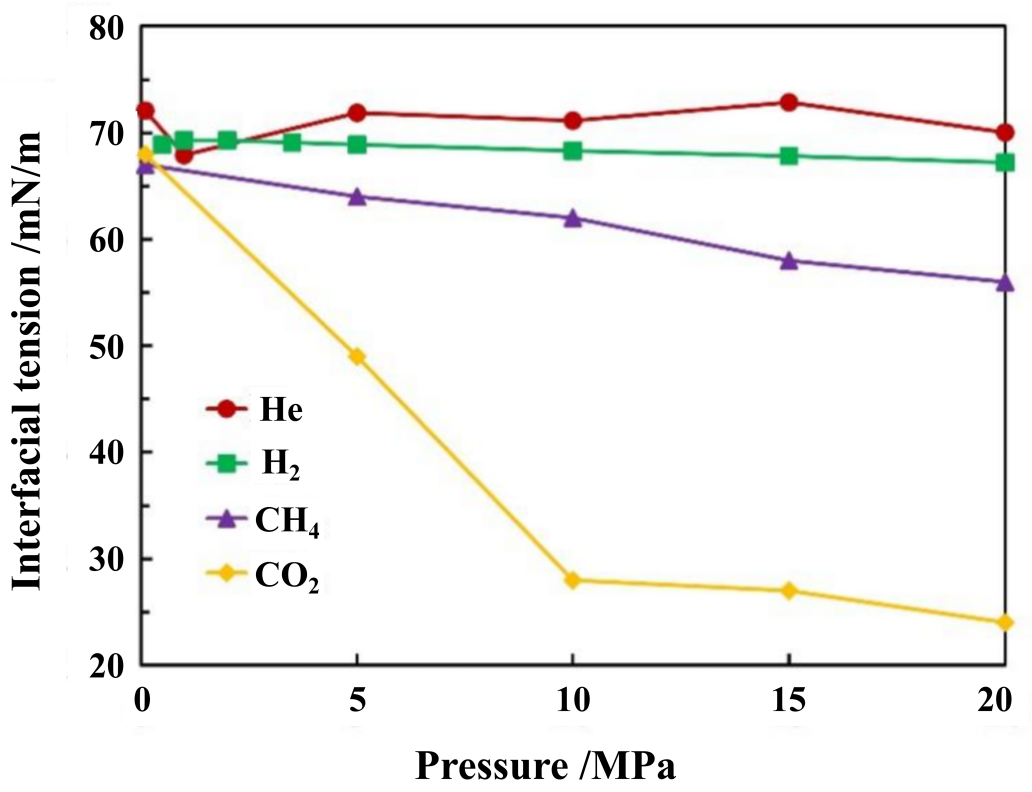

Fig. 2 Helium-water interfacial tension as a function of pressure, measured at 50 °C. Other interfacial tension data were collected from (Pan et al., 2021) for comparison

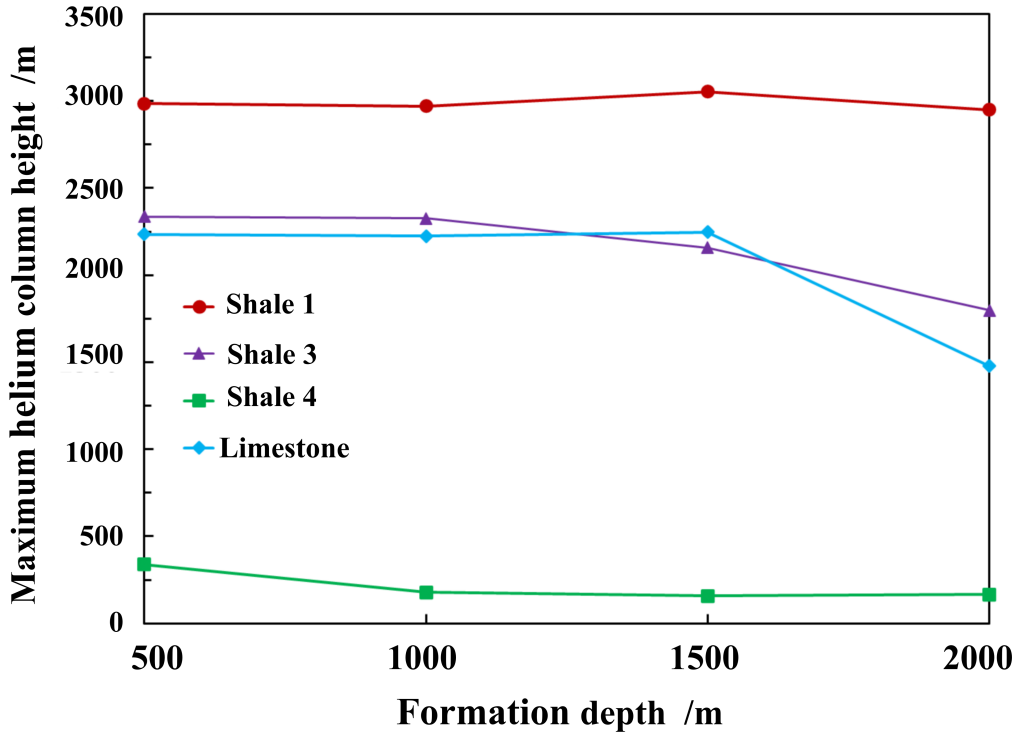

Fig. 3 Maximum helium column height which can be permanently immobilized beneath various caprocks as a function of formation depth (at 50 °C)

These results have clearly proved that helium and hydrogen have different wetting behaviors and it is not plausible to use helium to substitute hydrogen in the scenarios of underground hydrogen storage.

3.2 Helium-water interfacial tension

γ_{He-H_2O} fluctuated around 68–73 mN/m at 50 °C without any monotonous dependence on pressure (from 0.1 MPa to 20 MPa), Fig.2 and Tab.3. These values are close to $\gamma_{H_2-H_2O}$ and slightly larger than $\gamma_{CH_4-H_2O}$, while much larger than $\gamma_{CO_2-H_2O}$ at identical geo-storage conditions. Fundamentally, these differences are attributed to different intermolecular interactions between various gases and water (which are related to gas density; CO_2-water has a stronger affinity and lower interfacial tension because CO_2 density increases significantly with pressure) (Pan et al., 2021).

3.3 Maximum helium column height

h_{max} strongly depended on the caprock wettability, Figure 3. For example, at a representative storage formation depth of 1000 m, h_{max} was 2969, 180, 2325 and 2224 m, respectively for the completely water-wet shale 1, strongly water-wet shale 3, intermediate-wet shale 4 and strongly water-wet limestone. Furthermore, h_{max} decreased with storage formation depth, e.g., as the formation depth increased from 500 m to 2000 m, h_{max} decreased from 2984 m to 2949 m, from 2337 m to 1797 m, from 339 m to 166 m, and from 2235 m to 1479 m, respectively, for the above-mentioned three kinds of caprocks.

However, it is worthy to be emphasized that uncertainties may exist because

1) deionized water was used in the experiment, while at subsurface it is brine filled the porous rocks (Huppert & Neufeld, 2014);

2) a constant temperature of 50° was assumed for simplicity, while temperature varies with formation locations and depths (Wang et al., 2003);

3) the stored helium was assumed to exist as continuous plumes beneath the caprocks and the local heterogeneities were neglected.

4 Conclusions

Helium is a critical but non-renewable raw material, which has widespread applications in various advanced technology areas (Anderson, 2018; Hurd et al., 2012; Nuttall et al., 2012; Siddhantakar et al., 2023). To avoid any potential helium supply chain breakdown, it is necessary to store large amounts of helium in porous reservoirs (Tade, 1967), which is sealed by low-permeability caprocks. In this scenario, helium wettability of caprocks and helium-water interfacial tension are two key parameters to determine structural gas geo-storage capacity. However, experimental data about these two parameters at helium geo-storage conditions are seriously lacking. Therefore, we experimentally measured these two parameters across a range of rock compositions and theoretically estimated the corresponding geo-storage capacity. We demonstrated that

1) clay-rich shale caprocks ranged from completely to strongly water-wet, indicating high sealing efficiency;

2) organic-rich shale caprocks ranged from weakly water-wet to intermediate-wet, indicating poor sealing efficiency;

3) carbonate-rich caprocks ranged from strongly to weakly water-wet, indicating moderate sealing efficiency;

4) helium-water interfacial tension fluctuated around 68 – 73 mN/m, irrelevant of pressure changes;

5) maximum helium column height varied from 159 *m* to 3054 *m* depending on various caprock wettability and storage formation depth.

This work therefore provides fundamental data and scientific guidance for helium geo-storage in porous reservoirs, thus further enabling long-term helium supply-security worldwide. In terms of caprock screening, clay-rick caprocks with lean TOC is highly recommended because it can provide the strongest capillary sealing integrity, while clay swelling and crack may be induced during the cyclic helium injection and withdraw, thus leakage risks still exist. Future work will be focused on the coupling mechanisms of capillary and stress sealing integrity for clay-rich caprocks.

Acknowledgements

The authors would like to acknowledge the funding support from the MOST National Science and Technology Major Project (No. 2025ZD1406800), the Natural Science Foundation of China grant (No. 52304019 and W2521153), the CNPC Innovation Found (2023DQ02-0505), and the Science Foundation of China University of Petroleum - Beijing (No. ZX20250057). The Royal Society (Project Reference: IEC/NSFC/252203, held by Gang Wang) is gratefully acknowledged for supporting travel and collaborative activities related to this work. This project was also supported by Anhui Provincial Natural Science Foundation (Grant No. 2308085MA19).

Conflict of interest

The authors declare no competing interest.

References

Al-Yaseri AZ, Lebedev M, Barifcani A, et al. 2016. Receding and advancing (CO_2+ brine + quartz) contact angles as a function of pressure, temperature, surface roughness, salt type and salinity. *The Journal of Chemical Thermodynamics*, **93**: 416–423. doi:10.1016/j.jct.2015.07.031.

Anderson ST. 2018. Economics, Helium, and the U.S. Federal Helium Reserve: Summary and Outlook. *Natural Resources Research*, **27**: 455–477. doi:10.1007/s11053-017-9359-y.

Arif M, Lebedev M, Barifcani A, et al. 2017. Influence of shale-total organic content on CO_2 geo-storage potential. *Geophysical Research Letters*, **44**(17): 8769–8775. doi:10.1002/2017GL073532.

Ballentine CJ, Burnard PG. 2002. Production, Release and Transport of Noble Gases in the Continental Crust. *Reviews in Mineralogy and Geochemistry*, **47**: 481–538. doi:10.2138/rmg.2002.47.12.

Berry JD, Neeson MJ, Dagastine RR, et al. 2015. Measurement of surface and interfacial tension using pendant drop tensiometry. *Journal of Colloid and Interface Science*, **454**: 226–237. doi:10.1016/j.jcis.2015.05.012.

Cheng A, Lollar BS, Gluyas JG, et al. 2023. Primary N_2–He gas field formation in intracratonic sedimentary basins. *Nature*, **615**: 94–99. doi:10.1038/s41586-022-05659-0.

Espinoza DN, Santamarina JC. 2017. CO_2 breakthrough—Caprock sealing efficiency and integrity for carbon geological storage. *International Journal of Greenhouse Gas Control*, **66**: 218–229. doi:10.1016/j.ijggc.2017.09.019.

Gluyas J, Ballentine C, Danabalan D, et al. 2023. (How to explore for helium). *84th EAGE Annual Conference & Exhibition*, **2023**:1-6. doi:10.3997/2214-4609.2023101224.

Heinemann N, Alcalde J, Miocic JM, et al. 2021. Enabling large-scale hydrogen storage in porous media – the scientific challenges. *Energy & Environmental Science*, **14**: 853–864. doi:10.1039/D0EE03536J.

Hosseini M, Fahimpour J, Ali M, et al. 2022. Capillary Sealing Efficiency Analysis of Caprocks: Implication for Hydrogen Geological Storage. *Energy & Fuels*, **36**(7): 4065–4075. doi:10.1021/acs.energyfuels.2c00281.

Hosseini M, Sedev R, Ali M, et al. 2023. Hydrogen-wettability alteration of Indiana limestone in the presence of organic acids and nanofluid. *International Journal of Hydrogen Energy*, **48**(90): 35220–35228. doi:10.1016/j.ijhydene.2023.05.292.

Huppert HE, Neufeld JA. 2014. The Fluid Mechanics of Carbon Dioxide Sequestration. *Annual Review of Fluid Mechanics*, **46**: 255–272. doi:10.1146/annurev-fluid-011212-140627.

Hurd AJ, Kelley RL, Eggert RG, et al. 2012. Energy-critical elements for sustainable development. *MRS Bulletin*, **37**: 405–410. doi:10.1557/mrs.2012.54.

Iglauer S. 2017. CO_2–Water–Rock Wettability: Variability, Influencing Factors, and Implications for CO_2 Geostorage. *Accounts of Chemical Research*, **50**(3): 1134–1142. doi:10.1021/acs.accounts.6b00602.

Iglauer S, Ali M, Keshavarz A. 2021. Hydrogen Wettability of Sandstone Reservoirs: Implications for Hydrogen Geo-Storage. *Geophysical Research Letters*, **48**(3): e2020GL090814. doi:10.1029/2020GL090814.

Lander LM, Siewierski LM, Brittain WJ, et al. 1993. A systematic comparison of contact angle methods. *Langmuir*, **9**(8): 2237–2239. doi:10.1021/la00032a055.

Liang ZK, Jiang ZX, Li Z, et al. 2021. Investigation into the Pore Structure and Multifractal Characteristics of Shale Reservoirs through N_2 Adsorption: An Application in the Triassic Yanchang Formation, Ordos Basin, China. *Geofluids*, **2021**: 9949379. doi:10.1155/2021/9949379.

Nelson PH. 2009. Pore-throat sizes in sandstones, tight sandstones, and shales. *AAPG Bulletin*, **93**(3): 329–340. doi:10.1306/10240808059.

Nunn JA. 1996. Buoyancy-driven propagation of isolated fluid-filled fractures: Implications for fluid transport in Gulf of Mexico geopressured sediments. *Journal of Geophysical Research: Solid Earth*, **101**(B2): 2963–2970. doi:10.1029/95JB03210.

Nuttall WJ, Clarke RH, Glowacki BA. 2012. Stop squandering helium. *Nature*, **485**: 573–575. doi:10.1038/485573a.

Pan B, Li YJ, Wang HQ, et al. 2017. CO_2 and CH_4 Wettabilities of Organic-Rich Shale. *Energy & Fuels*, **32**(2): 1914–1922. doi:10.1021/acs.energyfuels.7b01147.

Pan B, Jones F, Huang ZQ, et al. 2019. Methane (CH_4) Wettability of Clay-Coated Quartz at Reservoir Conditions. *Energy & Fuels*, **33**(2): 788–795. doi:10.1021/acs.energyfuels.8b03536.

Pan B, Gong CP, Wang XP, et al. 2020. The interfacial properties of clay-coated quartz at reservoir conditions. *Fuel*, **262**: 116461. doi:10.1016/j.fuel.2019.116461.

Pan B, Li YJ, Zhang MS, et al. 2020. Effect of total organic carbon (TOC) content on shale wettability at high pressure and high temperature conditions. *Journal of Petroleum Science and Engineering*, **193**: 107374. doi:10.1016/j.petrol.2020.107374.

Pan B, Yin X, Ju Y et al. 2021. Underground hydrogen storage: Influencing parameters and future outlook. *Advances in Colloid and Interface Science*, **294**: 102473. doi:10.1016/j.cis.2021.102473.

Pan B, Clarkson CR, Atwa M, et al. 2021. Wetting dynamics of nanoliter water droplets in nanoporous media. *Journal of Colloid and Interface Science*, **589**: 411–423. doi:10.1016/j.jcis.2020.12.108.

Pan B, Clarkson CR, Atwa M, et al. 2021. Spontaneous Imbibition Dynamics of Liquids in Partially-Wet Nanoporous Media: Experiment and Theory. *Transport in Porous Media*, **137**: 555–574. doi:10.1007/s11242-021-01574-6.

Pan B, Liu K, Ren B, et al. 2023. Impacts of relative permeability hysteresis, wettability, and injection/withdrawal schemes on underground hydrogen storage in saline aquifers. *Fuel*, **333**: 126516. doi:10.1016/j.fuel.2022.126516.

Pan B, Song TR, Yue M, et al. 2024. Machine learning - based shale wettability prediction: Implications for H_2, CH_4 and CO_2 geo-storage. *International Journal of Hydrogen Energy*, **56**: 1384–1390. doi:10.1016/j.ijhydene.2023.12.298.

Pan B, Matamba T, Yin X, et al. 2025. Experimental Investigations of the Impact of H_2, He, CH_4, and CO_2 Exposure on Kerogen Adsorption, Wettability, and Geomechanical Characteristics at Geo-Storage Conditions. *SPE Journal*, **2025**: n. pag. doi:10.2118/225446-pa.

Rapatskaya LA, Tonkikh ME, Ustyuzhanin AO. 2020. Natural reservoir as a geological body for storing helium reserves. *IOP Conference Series: Earth and Environmental Science*, **408**: 012060. doi:10.1088/1755-1315/408/1/012060.

Siddhantakar A, Santillán-Saldivar J, Kippes T, et al. 2023. Helium resource global supply and demand: Geopolitical supply risk analysis. *Resources, Conservation and Recycling*, **193**: 106935. doi:10.1016/j.resconrec.2023.106935.

Song J, Zhang DX. 2023. Comprehensive Review of Caprock-Sealing Mechanisms for Geologic Carbon Sequestration. *Environmental Science & Technology*, **47**(1): 9–22. doi:10.1021/es301610p.

Tade MD. 1967. Helium Storage in Cliffside Field. *Journal of Petroleum Technology*, **19**(7): 885–888. doi:10.2118/1624-PA.

Wang LS, Chen L, Liu SW, et al. 2003. Characteristics of Geo-Temperature Gradient Distribution in the Kuqa Foreland Basin on the North Edge of the Tarim Basin, Western China. *Chinese Journal of Geophysics*, **46**(3): 575–581. doi:10.1002/cjg2.3375.